Human Gene Therapy

Antisense modulation of both exonic and intronic splicing motifs induces skipping of a DMD pseudoexon responsible for X-Linked Dilated Cardiomyopathy

Journal:	*Human Gene Therapy*
Manuscript ID:	HUM-2010-010
Manuscript Type:	Research Article
Date Submitted by the Author:	20-Jan-2010
Complete List of Authors:	Rimessi, Paola; University of Ferrara, Dept. of Experimental and Diagnostic Medicine, Sect. of Medical Genetics Fabris, Marina; University of Ferrara, Dept. of Experimental and Diagnostic Medicine, Sect. of Medical Genetics Bovolenta, Matteo; University of Ferrara, Dept. of Experimental and Diagnostic Medicine, Sect. of Medical Genetics Bassi, Elena; University of Ferrara, Dept. of Experimental and Diagnostic Medicine, Sect. of Medical Genetics Falzarano, Sofia; University of Ferrara, Dept. of Experimental and Diagnostic Medicine, Sect. of Medical Genetics Gualandi, Francesca; University of Ferrara, Dept. of Experimental and Diagnostic Medicine, Sect. of Medical Genetics Rapezzi, Claudio; University of Bologna and S.Orsola-Malpighi Hospital, Institute of Cardiology Coccolo, Fabio; University of Bologna and S.Orsola-Malpighi Hospital, Institute of Cardiology Perrone, Daniela; University of Ferrara, Dept. of Biology and Evolution Medici, Alessandro; University of Ferrara, Dept. of Biology and Evolution Ferlini, Alessandra; University of Ferrara, Dept. of Experimental and Diagnostic Medicine, Sect. of Medical Genetics
Keyword:	Muscle and Connective Tissue - Includes inherited, progressive and acquired diseases < C. Disease Models and Clinical Applications, D. Gene Regulation - Includes gene expression, animal model systems and gene modification


scholarONE
Manuscript Central

Antisense modulation of both exonic and intronic splicing motifs induces skipping of a *DMD* pseudoexon responsible for X-Linked Dilated Cardiomyopathy

Paola Rimessi (1), Marina Fabris (1), Matteo Bovolenta (1), Elena Bassi (1), Sofia Falzarano (1), Francesca Gualandi (1), Claudio Rapezzi (2), Fabio Coccolo (2) Daniela Perrone (3), Alessandro Medici (3), Alessandra Ferlini (1)

(1) Department of Molecular and Diagnostic Medicine, Section of Medical Genetics, University of Ferrara, Italy;
(2) Institute of Cardiology, University of Bologna and S.Orsola-Malpighi Hospital, Bologna, Italy;
(3) Department of Biology and Evolution, University of Ferrara, Italy.

Running title: Antisense modulation of a *DMD* pseudoexon

ABSTRACT

Antisense-mediated exon skipping has proven to be efficacious for subsets of Duchenne muscular dystrophy mutations. This approach is based on targeting specific splicing motifs that interferes with the spliceosome assembly by steric hindrance. Proper exon recognition by the splicing machinery is thought to depend on exonic splicing enhancer sequences, often characterized by purine rich stretches, representing potential targets for antisense-mediated exon skipping.

We identified and functionally characterized two purine-rich regions located within dystrophin intron 11 and involved in splicing regulation of a pseudoexon. A functional role of these sequences was suggested by a pure intronic *DMD* deletion causing X-linked dilated cardiomyopathy through the prevalent cardiac incorporation of the aberrant pseudoexon, marked as *Alu*-exon, into the dystrophin transcript.

The first splicing sequence is contained within the pseudoexon, while the second one is localised within its 3' intron. We demonstrated that the two sequences actually behave as splicing enhancers in cell-free splicing assays since their deletion strongly interferes with the pseudoexon inclusion.

Cell-free results were then confirmed in myogenic cells derived from the patient with X-linked dilated cardiomyopathy targeting the identified motifs with antisense molecules and obtaining a reduction in the dystrophin pseudoexon recognition.

The splicing motifs identified could represent target sequences for a personalized molecular therapy in this peculiar *DMD* mutation. Our results demonstrated for the first time the role of intronic splicing sequences in antisense modulation with implications in exon-skipping-mediated therapeutic approaches.

Keywords: dystrophin pseudoexon, X-linked dilated cardiomyopathy, splicing enhancer sequences, antinsense molecules, exon skipping

INTRODUCTION

Duchenne muscular dystrophy (DMD) is an X-linked inherited muscle degenerative disorder mainly caused by frame-disrupting mutations due to large rearrangements in the dystrophin gene (*DMD*) (Muntoni *et al.*, 2003; Aarstma-Rus *et al.*, 2006 a). The milder allelic form of the disease, Becker muscular dystrophy (BMD), is due to in frame mutations which preserve a shorter but functional protein. In this context, restoration of dystrophin synthesis via oligoribonucleotide

(AON)-mediated exon skipping represents a possible therapeutic approach, converting a DMD to a BMD phenotype, potentially suitable for up to 90% of DMD patients (Aarstma-Rus *et al.*, 2004).

Currently, due to improvements in direct sequencing and dosage methodologies, dystrophinopathy detection rate via genomic DNA analysis is about 93-96%.

Furthermore, the recent implementation of high-throughput platforms has become feasible the recognition of a previously difficult to identify category of *DMD* mutations, represented by deep intronic mutations. These rare mutations often create novel splice sites, resulting in the inclusion of intronic sequences as a pseudoexon within the mRNA. A recent paper describes the modulation of two different *DMD* mutations, causing BMD and DMD phenotypes, by the AON-mediated pseudoexon skipping, demonstrating the feasibility of this approach for this class of mutations (Tuffery-Giraud *et al*., 2003; Beroud *et al*., 2004; Gurvich *et al.*, 2008). Notably, a therapy based on pseudoexon skipping could be particularly beneficial, as the resultant rescued dystrophin is a wild type, not internally deleted protein.

Several examples have clearly demonstrated that deep intronic mutations may affect the pre-mRNA splicing process in a number of disease-associated genes (Highsmith *et al.*, 1994; Metherell *et al.*, 2001; Pagani *et al.*, 2002).

Exon recognition is defined through consensus sequences at the 5' splice site, the 3' splice site and associated polypirimidine tract, and the branch point sequence. The selection of an exon is further determined by RNA *cis* elements generally referred to as exonic or intronic splicing enhancers (ESEs or ISEs) and exonic or intronic splicing silencers (ESSs or ISSs).

The binding of splicing factors, such as serine/arginine rich proteins (SR proteins), to sequences classified as splicing enhancers, and the subsequent recruitment of other essential splicing factors to the splice sites result in the exon inclusion into the mRNA (Valcarcel and Green, 1996; Chandler *et al*., 1997; Mayeda *et al*., 1999; Smith and Valcarcel, 2000; Lam and Hertel, 2002; Zheng, 2004; Lewandowska *et al*., 2005; Buratti *et al*., 2006). As SR protein binding to ESEs is essential for exon inclusion, blocking ESEs with AONs would be expected to result in exon skipping (Sazani and Kole, 2003; Baralle and Baralle, 2005; Aarstma -Rus and van Ommen, 2007; Wilton et al., 2007; Solis et al., 2008).

Alternatively spliced exons contain more then one regulatory *cis* element in the exon and/or in the flanking introns, and inclusion or skipping of the exon is determined by the activity of several proteins associated with these elements (Smith and Valcarcel, 2000; Black, 2003). Tissue specific splicing patterns are thought to be determined by subtle changes in the proportion of SR proteins present in different cell types (Caceres *et al*., 1994; Zhu *et al*., 2001; Qi *et al*., 2006) and by the tissue-restricted expression of *trans*-acting factors that specifically interact with intronic regulatory

cis elements (ISE/ISS), as recently described for the recognition of the rat FGFR2 exon IIIc in mesenchymal cells (Seth *et al.,* 2008).

In a previous work we described a splicing mutation occurring in a patient with X-linked dilated cardiomyopathy (XLDC) (Ferlini *et al*., 1998; Rimessi *et al*., 2005). This mutation determined the tissue-specific inclusion of an out-of-frame pseudoexon (*Alu*-exon) into the dystrophin transcript with the co-existence of wild-type and mutated transcripts in skeletal muscle, and the exclusive presence of the aberrant transcript in the heart, giving rise to the XLDC phenotype (Gualandi *et al.*, 2003; Cohen *et al*., 2004).

Here we show that *Alu*-exon recognition is strongly downregulated by the deletion of two predicted splicing motifs in cell-free splicing assays and by the competition with antisense molecules in cell cultures, underlining the importance of local sequence analysis for developing therapies to turn off activated pseudoexons. Selective targeting of these sequences using AONs induced a partial restoration of wild-type splicing, showing that the XLDC mutation has the potential to be rectified by antisense gene therapy. This is the first report of XLDC pseudoexon modulation by targeting both exonic and intronic splicing motifs, with obvious implications in designing AONs mediated therapies.

MATERIALS AND METHODS

Mini-genes for *in vitro* transcription

All the constructs used in this study were prepared using standard cloning techniques (Sambrook *et al*., 1989). The sequences of the oligonucleotides used for the experimental procedures are reported in Table 1. A graphic representation of the mutated dystrophin region is shown in Figure 1 A.

The sequence and orientation of the inserts of all the recombinant plasmids (Gualandi *et al.*, 2003) were verified by double-strand DNA sequencing. The entire sequence of each insert was determined on both directions using fluorescent dideoxynucleotidetriphosphates (Applied Biosystems) and an automated DNA sequencer (ABIPRISM 3130, Applied Biosystems).

Three mini-genes were designed (Fig. 1 B, C, D).

In vitro transcription and splicing assays

The templates for *in vitro* transcription reactions were obtained by PCR amplification of the mini-genes using the forward primer T7Ex2 which contains the T7 promoter sequence, and the reverse primer Ex3R (Table 1), as previously described (Gualandi *et al.*, 2003).

In vitro splicing reactions were carried out according to previously reported procedures (Eperon *et al*., 2000) using HeLa cell nuclear extracts (Computer Cell Culture Centre, Belgium). The products of the splicing reactions were resolved by electrophoresis through a denaturing (8 M Urea) polyacrylamide gel (5%), and visualized by exposure to a BioMax X-ray film (Kodak) using an intensifying screen.

RT-PCR of splicing products

Following autoradiography, slices of the dried gel containing RNA splicing products were excised and incubated overnight in SDS buffer at 4°C. The eluted RNA products were recovered by ethanol precipitation and used as templates for cDNA synthesis. Reverse transcription (RT) was performed with random hexanucleotide primers and the SUPERSCRIPT™ II Reverse transcriptase (Life Technologies) as previously described (Muntoni *et al*., 1995). cDNAs were amplified using as primers the oligonucleotides Ex2F and Ex3R. These oligonucleotides map to sequence segments of exon 2 and exon 3 of the rabbit β-globin gene flanking the splicing constructs (Table 1).

The M3 transcript was characterized by sequencing the RT-PCR product obtained using the oligonucleotides Ex2F and Ex3R (Table 1).

AONs design and synthesis

AONs design was based on in silico analysis of dystrophin intron 11 mutated sequence using the ESE finder algorithm to identify regulatory motifs involved in exon definition, and the M-FOLD program to predict mRNA secondary structure (Aarstma-Rus et al., 2006 b) (Table 2).

The synthesised AONs contain a full-length phosphorothioate backbone and 2'-O-methyl modified ribose molecules. Oligonucleotides synthesis was carried out on an ÄKTA™ oligopilot plus 10 DNA/RNA synthesizer (GE Healthcare) as described (Rimessi *et al.*, 2009).

Myogenic cell cultures and AONs transfection

Primary human fibroblasts from the XLDC patient were isolated from a skin biopsy (obtained after informed consent for research purposes, Ethical Approval N. 9/2005). Cells were grown in high-glucose DMEM (GIBCO), supplemented with 20% foetal bovine serum (FBS; GIBCO) and antibiotic/antimicotic solution (Sigma). Myogenesis was induced by infection with an Ad5-derived, EA1-deleted adenoviral vector carrying the MyoD gene as previously described [3]. Myotubes obtained after 7-10 days of culture in differentiation medium (2% FBS) were transfected with AONs (100 nM) in presence of polyethylenimine (ExGen500, MBI Fermentas) (2 μl per μg of

AON) as transfection reagent, according to the manufacturer's instruction. For ESEN2 and SRBN3 50 nM and 75 nM concentrations were also tested.

Immunofluorescence analysis

48 hours after AON treatment, myotube cultures grown onto cover-slips were rapidly washed with phosphate buffer saline (PBS) and fixed with cold methanol for 7 minutes. Samples were saturated with 4% bovine serum albumin (BSA) phosphate buffer saline (PBS) solution for 30 minutes and double-labeled with mouse monoclonal antibodies against desmin or developmental myosin heavy chain (Novocastra Laboratories Ltd), diluted 1:10 and 1:60 respectively, or polyclonal antibody against dystrophin H300 (Santa Cruz, 1:100). After several washing with PBS, samples were incubated with FITC/TRITC-conjugated secondary antibodies diluted 1:100 for 1h (DAKO). The slides were mounted with ProLong Antifade reagent (Molecular Probe) and observed using a Nikon Eclipse 80i fluorescence microscope.

RNA analysis

48 hours after transfection, total RNA was isolated from myotube cultures (RNeasy Kit Qiagen) and reverse transcribed into cDNA using the high capacity cDNA reverse transcription kit (Applied Biosystems) with random primers. RT-PCR was performed on β-actin (primers sequences available upon request) to verify cDNA synthesis and on dystrophin (10F 5'-tggaagctcctgaagacaagtc-3' and M12 5'- gattctggagatccattaaaactct-3') to analyse the relative amount of skipped/not skipped transcripts (399 and 558 bp, respectively).

To precisely quantify both the percentage of skipping of the *Alu*-exon and the amount of dystrophin transcript, we developed exon-specific realtime assays detecting the "aberrant" exon and the human dystrophin exons 10 and 12. These exons were chosen because not involved in spontaneous alternative splicing events in humans. Real time assays on exons 10 and 12 were used as reference to quantify the amount of physiological pseudoexon skipping and percentage of induced pseudoexon skipping in treated cells compared to untreated cells (internal reference). The same exons, 10 and 12 , were used as target to quantify dystrophin transcript level with β-actin transcript (β-actin gene, Applied Biosystems) as reference, in AON-treated, not treated XLDC patient myogenic cells, in comparison to myogenic cells from a healthy donor (cutaneous fibroblast MyoD induced). Real time assays are based on TaqMan MGB technology and have been designed by PrimerExpress Applied Biosystems software (primer and probe sequences are available upon request). The amount of the target sequences in respect to internal references (represented by adjacent dystrophin exon) and to an appropriate endogenous control (β-actin gene)

was evaluated by the comparative CT method in respect to the untreated control (ΔΔCt Method) (Applied Biosystems User Bullettin #2).

RESULTS

Cell-free splicing assays

In order to functionally characterize the two purine rich regions contained in the *Alu*-exon, three splicing constructs were set up (Fig. 1). MUA mini-gene contains the rearranged XLDC genomic region of the dystrophin intron 11, including the *Alu*-exon, the two cryptic splice sites, the putative branchpoint, and the intronic purine rich region, named SRB motif (Fig. 1 A and B). MUAΔE and MUAΔSRB represent deletion constructs.

MUA-ΔE mini-gene, obtained from the MUA, lacks the purine rich exonic motif (ESE), and maintains the *Alu*-exon, the two cryptic splice sites, the putative branchpoint, and the SRB motif (ISE) (Fig. 1 A and C).

The MUA-ΔSRB mini-gene was generated by replacing the SRB region of the MUA mini-gene with a neutral sequence of similar length from phage λ in order to avoid length-related artefacts (Fig. 1 D).

All the constructs were assayed in *in vitro* splicing assays.

The MUA mini-gene *in vitro* splicing assay shows the rabbit β-globin canonical products (B1 and B2) detected after 30 min of incubation, despite of the relevant size of the transcript (1372 bp). The fragment of 437 bp (M2) corresponding to a splicing product incorporating the *Alu*-exon between rabbit β-globin exon 2 and exon 3 was detected after 1 hr and its relative abundance increased with time (Fig. 2 A).

MUA-ΔE mini-gene splicing assay showed, in addition to the β-globin canonical splicing products, a low abundance novel 344 bp transcript (M3), visible at 2 and 3 hours of incubation time (Fig. 2 A). Sequence analysis of this fragment revealed that it represents a splicing product incorporating a novel 66 bp exon defined by the activation of two different splice sites: a 3' cryptic splice located 4 bp downstream the 3' splice site used by the *Alu*-exon and a 5' cryptic splice site, located 74 bp upstream the one used by the *Alu*-exon (Fig. 1 A). Notably, no M2 splicing product was detected in the MUA-ΔE mini-gene splicing assay at any time point.

The comparison of the parental MUA mini-gene with the deleted MUA-ΔE in different splicing assays demonstrated that the deletion of the ESE motif abolished the *Alu*-exon definition (Fig. 2 A).

In order to test the involvement of the SRB motif in the *Alu*-exon recognition, we assayed the splicing behavior of the MUA-ΔSRB mini-gene. In addition to the β-globin canonical products, only a splicing product referred to as M4 was detected. M4 corresponded to an aberrant β-globin transcript containing exon 2 joined to two copies of exon 3 (Fig. 2 B). The deletion of the SRB region therefore abolished the *Alu*-exon inclusion.

Immunofluorescence analysis of MyoD transformed fibroblasts

Since muscle biopsy suitable for cell culture was not available, patient skin derived fibroblasts were converted into myogenic cells by infection with a replication-defective adenovirus encoding MyoD.

Immunofluorescence analysis of desmin and myosin, two protein specifically expressed in muscle tissue, was performed to define the differentiation stage of the Myo-D transformed fibroblasts. We detected expression of desmin and myosin in patient derived myogenic cultures, therefore confirming myogenic conversion (Fig. 3).

Dystrophin expression was detected both in AONs treated and untreated patient derived myogenic cells, correctly localized at the sarcolemma, resembling the XLDC patient's skeletal muscle behavior. However, it was not possible to accurately quantify an increased expression of the protein in AON treated cells (Fig. 4).

Splicing modulation by AONs in patient's derived myogenic cells

An analysis performed with the Human Splicing Finder tool (Desmet *et al*., 2009) revealed that the two regulatory sequences (ESE and ISE) correspond to overlapping enhancers (Tra2ß and 9G8 motifs) and silencers (hnRNPA1 motifs) motifs potentially explaining the tissue-specific splicing pattern. AONs directed at predicted ESE/ISE motifs were evaluated for their potential to induce targeted *Alu*-exon skipping at concentration of 100 nM. Cultured patient's myogenic cells were transfected with the different designed AONs (Table 2) and analyzed for *Alu*-exon skipping.

RT-PCR amplification of AON-treated or untreated patient derived cells using oligonucleotides on dystrophin exon 10 and 12 generated a mixture of two products: one corresponding to the wild-type transcript and a second larger fragment containing the cryptic exon. The comparison of the relative abundance of the two products in treated and untreated cells demonstrated that AONs specifically targeting the ESE motif (ESEN1 and ESEN2) induced an increased ratio of the correct transcript, while AONs directed at the ISE domain appeared less effective (data not shown). Sequence analysis confirmed the correct 11-12 exons junction.

AON-induced skipping efficiency, was estimated by ESRA on *Alu*-exon, using both adjacent dystrophin exons (10 and 12) and beta-actin as references, in treated compared to untreated cells (Fig 5 A). The percentage of exon skipping varied considerably with a consistent increase when using ESEN1 and ESEN2 (10,9 % and 11,06 %, respectively), while AONs directed against the ISE motif were less effective (5% skipping with SRBN3, 1,8 % with SRBN4, 2 % with SRBN5, 1,2 % using SRBV1 and 0,8 % using SRBV2), furthermore SRBN1and SRBN2 were unable to induce any detectable skipping.

The two more effective AONs, ESEN2 and SRBN3, worked at almost all concentrations tested in excluding *Alu*-exon from the mature transcript. The effect was shown to be concentration-dependent, with approximately 6,22% induced skipping at 50 nM, 10,24% at 75 nM, 11,08% at 100 nM ESEN2 and approximately 0,82% at 50 nM, 2,08% at 75 nM, 6% at 100 nM SRBN3 (Fig. 5 B). Treating patient derived cells with different combinations of these two AONs an additive action was excluded (data not shown).

Importantly, treating patient's cells with effective AONs resulted in a 2 to 3 folds increase of dystrophin transcription level (as detected by ESRA), in respect to myogenic cells from healthy donors, considered an added value due to the low basal level detected in these cells (20% of control cells).

DISCUSSION

We identified and functionally characterized two purine-rich regions located within dystrophin intron 11 putatively involved in splicing regulation of a pseudoexon which causes an XLDC phenotype. The splicing behavior of the dystrophin transcript due to the large pure intronic deletion resulted in the inclusion of this aberrant pesudoexon into the dystrophin transcript (Gualandi *et al.*, 2003). Skeletal muscles can produce both wild type and out-of-frame transcript, while cardiac tissue produces only the transcript including the *Alu*-exon, therefore accounting for dystrophin full deficiency (Ferlini *et al.*, 1998).

In order to address both the pseudoexon splicing regulation and its propensity to antisense-mediated exon-skipping we set up first a cell-free splicing assay using constructs with artificial deletions of the putative exonic or intronic splicing motifs, and then we modulated these motifs by a large number of AONs in myogenic cells derived from the XLDC patient.

Our studies demonstrated that the two predicted splicing motifs are actually involved in the pseudoexon recognition and therefore their targeting by AONs induces a reduction of the *Alu*-exon incorporation.

One of the two identified motifs consists of an exonic 11 bp purine stretch identified by comparative analysis with other known ESEs, that revealed only 2 different nucleotides between *Alu*-exon ESE and the well characterised SMN1 exon 7 ESE motif (insertion of two As in bold; SMN1 AAAGAAGGA; *Alu*-exon AAAGAA**AA**GGA/). It is relevant to underline that both the hexamers GAAGGA (SMN exon 7 ESE) and AAAGGA (*Alu*-exon ESE) do maintain the GGA triplet and belong to the same ESE consensus (Hofmann and Wirth, 2002; Singh *et al.*, 2004). This consensus is referred as 3D/5C in Fairbrother and colleagues paper, and is capable of acting at both 5' and 3' splice sites (Bourgeois *et al.*, 1999; Fairbrother *et al.*, 2002). Our cell-free results indicate that the *Alu*-exon ESE, similarly to the SMN1 exon 7 ESE, acts by activating both 3' and 5' splice sites.

Eperon and colleagues reported the characterization in mice cells of a splicing silencer located within the *Alu*-exon (Nasim *et al.*, 2003). They hypothesized that this motif may act differently in the heart and in skeletal muscles, therefore accounting for the tissue-specific expression of the XLDC mutation in this family, underlining the complexity of tissue specific exon choice known to involve multiple *cis* elements and *trans* factors (Tarn, 2007).

The second splicing sequence (SRB) we identified represents an intronic GA-rich stretch located downstream the 5' cryptic splice site of the alternative *Alu*-exon. Deletion of the SRB region in the mini-gene abolished the *Alu*-exon inclusion, suggesting it could act as an ISE sequence.

The bioinformatic analysis (Desmet *et al*., 2009) revealed that indeed the two regulatory sequences, *Alu*-exon ESE and SRB, correspond to overlapping enhancers (Tra2ß and 9G8 motifs) and silencers (hnRNPA1 motifs), suggesting that the level of expression of these key proteins in different tissues could explain the tissue-specific splicing pattern observed in the XLDC patient, as in general described in many reports (Barnard *et al*., 2002; Tran *et al*., 2003; Fisher *et al*., 2004; Qi *et al*., 2006).

The enhancer activity of these two splicing sequences was also confirmed by the results we obtained by AONs modulation in myogenic cells. Only targeting the *Alu*-exon ESE succeeded in inducing a significant percentage (10-12%) of exon skipping, therefore confirming that this ESE could represent an effective target for inhibiting the *Alu*-exon recognition.

When targeting by AONs the intronic splicing enhancer we obtained again an increased skipping of the *Alu*-exon (6%), once more suggesting a possible cooperative action between the two splicing sequences.

Dystrophin pseudoexons modulation by AONs has been recently described (Gurvich *et al*., 2008; Madden *et al*., 2009). Differently from the present work, in both cases the AONs treatment was performed in myogenic cells derived from muscle biopsies and targeting exonic sequences.

To our knowledge this is the first example of both pseudoexon modulation in MyoD-transformed fibroblasts and AONs-mediated exon skipping targeting an ISE. In fact, we were able to reproduce in cells from the XLDC patient's skin biopsy the same dystrophin splicing pattern we observed in the patient skeletal muscles, and therefore to use these cells for testing AONs versus both ESE and ISE sequences. ISE sequences targeting represents a novelty, in fact these motifs have not been subjected to the same extensive analysis as ESEs, and our current understanding of ISEs and the mechanisms by which they exert their effects is still incomplete.

In addition, we demonstrated that dystrophin mRNA level increases 2-3 folds in response to AONs treatment in patient's myogenic cells, suggesting that AON-induced pseudoexon skipping, while enhancing mRNA stability may increase the abundance of wild type transcript.

In conclusion, we demonstrated that both an exonic and an intronic splicing region act as enhancers for pseudoexon recognition, and that their modulation by AONs can reduce the *Alu*-exon incorporation within the dystrophin transcript, therefore offering therapeutic perspective for this peculiar mutation. Development of pseudoexon skipping therapies represents a type of personalized medicine directed at individual patients with private mutations.

Interestingly, although it is not surprising that the deletion/targeting of an ESE can strongly affect the exon definition process, the effect on splicing we observed after the deletion of the ISE region or its targeting by AONs is less obvious. As a consequence, it may be relevant to carefully consider the flanking intronic regions, instead of (or additionally to) using AONs cocktails, to induce specific exon skipping when targeting dystrophin exons considered poorly or even not-skippable (Errington *et al*., 2003; Wilton *et al*., 2007). Furthermore, AONs designed using criteria widely described (Aarstma-Rus *et al*., 2009), may greatly vary both in efficiency and in efficacy depending on the intronic mutation breakpoints, and consequently on the loss/maintenance of intronic splicing regulatory sequences. Considering our results we think that this issue deserves to be further studied.

ACKNOWLEDGEMENTS

This works was fully supported by Telethon Italy Foundation (Grants GGP5115 and GUP0711 to AF).

REFERENCES

1. AARTSMA-RUS, A., JANSON, A.A., HEEMSKERK, J.A., DE WINTER, C.L., VAN OMMEN, G.J., VAN DEUTEKOM, J.C. (2006) Therapeutic modulation of DMD splicing by blocking exonic splicing enhancer sites with antisense oligonucleotides. Ann. N. Y. Acad. Sci. 1082, 74-76.
2. AARTSMA-RUS, A., JANSON, A.A., KAMAN, W.E., BREMMER-BOUT, M., VAN OMMEN, G.J., DEN DUNNEN, J.T., VAN DEUTEKOM, J.C.. (2004) Antisense-induced multiexon skipping for Duchenne muscular dystrophy makes more sense. Am. J. Hum. Genet. 74, 83–92.
3. AARTSMA-RUS, A., VAN DEUTEKOM, J.C., FOKKEMA, I.F., VAN OMMEN, G.J., DEN DUNNEN, J.T. (2006) Entries in the Leiden Duchenne muscular dystrophy mutation database: an overview of mutation types and paradoxical cases that confirm the reading-frame rule. Muscle Nerve. 34, 135-144.
4. AARTSMA-RUS, A., VAN OMMEN, G.J. (2007) Antisense-mediated exon skipping: a versatile tool with therapeutic and research applications. RNA. 13, 1609-1624.
5. AARTSMA-RUS, A., VAN VLIET, L., HIRSCHI, M., JANSON, A.A., HEEMSKERK, H., DE WINTER, C.L., DE KIMPE, S., VAN DEUTEKOM, J.C., 'T HOEN, P.A, VAN OMMEN, G.J. (2009) Guidelines for antisense oligonucleotide design and insight into splice-modulating mechanisms. Mol. Ther. 17, 548-553.
6. BARALLE, D., BARALLE, M. (2005) Splicing in action: assessing disease causing sequence changes. J. Med. Genet. 42, 737-748.
7. BARNARD, D.C., LI, J., PENG, R., PATTON, J.G. (2002) Regulation of alternative splicing by SRrp86 through coactivation and repression of specific SR proteins. RNA. 8, 526-533.
8. BÉROUD C, CARRIÉ A, BELDJORD C, DEBURGRAVE N, LLENSE S, CARELLE N, PECCATE C, CUISSET JM, PANDIT F, CARRÉ-PIGEON F, MAYER M, BELLANCE R, RÉCAN D, CHELLY J, KAPLAN JC, LETURCQ F. (2004)

Dystrophinopathy caused by mid-intronic substitutions activating cryptic exons in the DMD gene. Neuromuscul. Disord. 14, 10-18.

9. BLACK, D.L. (2003) Mechanisms of alternative pre-messenger RNA splicing. Annu. Rev. Biochem. 72, 291-336. Review.
10. BOURGEOIS, C.F., POPIELARZ, M., HILDWEIN, G., STEVENIN, J. (1999) Identification of a bi-directional splicing enhancer: differential involvement of SR proteins in 5' or 3' splice site activation. Mol. Cell. Biol. 19, 7347-7356.
11. BURATTI, E., BARALLE, M., BARALLE, F.E. (2006) Defective splicing, disease and therapy: searching for master checkpoints in exon definition. Nucleic Acids Res. 34, 3494-3510.
12. CACERES, J.F., STAMM, S., HELFMAN, D.M., KRAINER, A.R. (1994) Regulation of alternative splicing in vivo by overexpression of antagonistic splicing factor. Science. 265, 1706-1709.
13. CHANDLER, S.D., MAYEDA, A., YEAKLEY, J.M., KRAINER, A.R., FU, X.D. (1997) RNA splicing specificity determined by the coordinated action of RNA recognition motifs in SR proteins. Proc. Natl. Acad. Sci. U.S.A. 94, 3596-3601.
14. COHEN, N., RIMESSI, P., GUALANDI, F., FERLINI, A., MUNTONI, F. (2004) In vivo study of an aberrant dystrophin exon inclusion in X-linked dilated cardiomyopathy. Biochem. Biophys. Res. Commun. 317, 1215-1220.
15. DESMET, F.O., DESMET, F.O., HAMROUN, D., LALANDE, M., COLLOD-BÉROUD, G., CLAUSTRES, M., BÉROUD, C. (2009) Human Splicing Finder: an online bioinformatics tool to predict splicing signals. Nucleic Acids Res. 37, e67.
16. EPERON, I.C., MAKAROVA, O.V., MAYEDA, A., MUNROE, S.H., CÁCERES, J.F., HAYWARD, D.G., KRAINER, A.R. (2000) Selection of alternative 5' splice sites: role of U1 snRNP and models for the antagonistic effects of SF2/ASF and hnRNP A1. Mol. Cell. Biol. 20, 8303-8318.
17. ERRINGTON, S.J., MANN, C.J., FLETCHER, S., WILTON, S.D. (2003) Target selection for antisense oligonucleotide induced exon skipping in the dystrophin gene. J. Gene Med. 5, 518-527.
18. FAIRBROTHER, W.G., YEH, R.F., SHARP, P.A., BURGE, C.B. (2002) Predictive identification of exonic splicing enhancers in human genes. Science. 297, 1007-1103.
19. FERLINI, A., GALIE, N., MERLINI, L., SEWRY, C., BRANZI, A., MUNTONI, F. (1998) A novel Alu-like element rearranged in the dystrophin gene causes a splicing

mutation in a family with X-linked dilated cardiomyopathy. Am. J. Hum. Genet. 63, 436-446.

20. FISCHER, D.C., NOACK, K., RUNNEBAUM, I.B., WATERMANN, D.O., KIEBACK, D.G., STAMM, S., STICKELER, E. (2004) Expression of splicing factors in human ovarian cancer. Oncol. Rep. 11, 1085-1090.
21. GUALANDI, F., TRABANELLI, C., RIMESSI, P., CALZOLARI, E., TOFFOLATTI, L., PATARNELLO, T., KUNZ, G., MUNTONI, F., FERLINI, A. (2003) Genomic definition of a pure intronic dystrophin deletion responsible for an XLDC splicing mutation: in vitro mimicking and antisense modulation of the splicing abnormality. Gene. 311, 25-33.
22. GURVICH, O.L., TUOHY, T.M., HOWARD, M.T., FINKEL, R.S., MEDNE, L., ANDERSON, C.B., WEISS, R.B., WILTON, S.D., FLANIGAN, K.M. (2008) DMD pseudoexon mutations: splicing efficiency, phenotype, and potential therapy. Ann. Neurol. 63, 81-89.
23. HIGHSMITH WE, BURCH LH, ZHOU Z, OLSEN, J.C., BOAT, T.E., SPOCK, A., GORVOY, J.D., QUITTELL, L., FRIEDMAN, K.J., SILVERMAN, L.M., BOUCHER, R.C.,.KNOWLES, M.R. (1994) A novel mutation in the cystic fibrosis gene in patients with pulmonary disease but normal sweat chloride concentrations. N. Engl. J. Med. 331, 974-980.
24. HOFMANN, Y., WIRTH, B. (2002) hnRNP-G promotes exon 7 inclusion of survival motor neuron (SMN) via direct interaction with Htra2-beta1. Hum. Mol. Genet. 11, 2037-2049.
25. LAM, B.J., HERTEL, K.J. (2002) A general role for splicing enhancers in exon definition. RNA. 8, 1233-1241.
26. LEWANDOWSKA, M.A., STUANI, C., PARVIZPUR, A., BARALLE, F.E., PAGANI, F. (2005) Functional studies on the ATM intronic splicing processing element. Nucleic Acids Res. 33, 4007-4015.
27. MADDEN, H.R., FLETCHER, S., DAVIS, M.R., WILTON, S.D. (2009) Characterization of a complex Duchenne muscular dystrophy-causing dystrophin gene inversion and restoration of the reading frame by induced exon skipping. Hum. Mutat. 30, 22-28.
28. MAYEDA, A., SCREATON, G.R., CHANDLER, S.D., FU, X.D., KRAINER, A.R. (1999) Substrate specificities of SR proteins in constitutive splicing are determined by

their RNA recognition motifs and composite pre-mRNA exonic elements. Mol. Cell. Biol. 19, 1853-1863.

29. METHERELL, L.A., AKKER, S.A., MUNROE, P.B., ROSE, S.J., CAULFIELD, M., SAVAGE, M.O., CHEW, S.L., CLARK, A.J. (2001). Pseudoexon activation as a novel mechanism for disease resulting in atypical growth-hormone insensitivity. Am. J. Hum. Genet. 69, 641-646.
30. MUNTONI, F., MELIS, M.A., GANAU, A., DUBOWITZ, V. (1995) Transcription of the dystrophin gene in normal tissues and in skeletal muscle of a family with X-linked dilated cardiomyopathy. Am. J. Hum. Genet. 56, 151-157.
31. MUNTONI, F., TORELLI, S., FERLINI, A. (2003) Dystrophin and mutations. One gene, several proteins, multiple phenotypes. Lancet Neurol. 2, 731-740.
32. NASIM, M.T., CHERNOVA, T.K., CHOWDHURY, H.M., YUE, B.G., EPERON, I.C. (2003) hnRNP G and Tra2beta: opposite effects on splicing matched by antagonism in RNA binding. Hum. Mol. Genet. 12, 1337-1348.
33. PAGANI, F., BURATTI, E., STUANI, C., BENDIX, R., DÖRK, T., BARALLE, F.E. (2002) A new type of mutation causes a splicing defect in ATM. Nat. Genet. 30, 426-429.
34. QI, J., SU, S., MCGUFFIN, M.E., MATTOX, W. (2006) Concentration dependent selection of targets by an SR splicing regulator results in tissue-specific RNA processing. Nucleic Acids Res. 34, 6256-6263.
35. RIMESSI, P., GUALANDI, F., DUPREZ, L., SPITALI, P., NERI, M., MERLINI, L., CALZOLARI, E., MUNTONI, F., FERLINI, A. (2005) Genomic and transcription studies as diagnostic tools for a prenatal detection of X-linked dilated cardiomyopathy due to a dystrophin gene mutation. Am. J. Med. Genet. A. 132, 391-394.
36. RIMESSI, P., SABATELLI, P., FABRIS, M., BRAGHETTA, P., BASSI, E., SPITALI, P., VATTEMI, G., TOMELLERI, G., MARI, L., PERRONE, D., MEDICI, A., NERI, M., BOVOLENTA, M., MARTONI, E., MARALDI, N.M., GUALANDI, F., MERLINI, L., BALESTRI, M., TONDELLI, L., SPARNACCI, K., BONALDO, P., CAPUTO, A., LAUS, M., FERLINI, A. (2009) Cationic PMMA nanoparticles bind and deliver antisense oligoribonucleotides allowing restoration of dystrophin expression in the mdx mouse. Mol. Ther. 17, 820-827.
37. SAMBROOK, J., FRITSCH, E.F., MANIATIS, T. (1989) Molecular Cloning: A Laboratory Manual. Cold Spring Harbor Laboratory Press, Cold Spring Harbor, NY.

38. SAZANI, P., KOLE, R. (2003) Therapeutic potential of antisense oligonucleotides as modulators of alternative splicing. J. Clin. Invest. 112, 481-486.
39. SETH, P., MILLER, H.B., LASDA, E.L., PEARSON, J.L., GARCIA-BLANCO, M.A. (2008) Identification of an intronic splicing enhancer essential for the inclusion of FGFR2 exon IIIc. J. Biol. Chem. 283, 10058-10067.
40. SINGH, N.N., ANDROPHY, E.J., SINGH, R.N. (2004) An extended inhibitory context causes skipping of exon 7 of SMN2 in spinal muscular atrophy. Biochem. Biophys. Res. Commun. 315, 381-388.
41. SMITH, C.W., VALCARCEL, J. (2000) Alternative pre-mRNA splicing: the logic of combinatorial control. Trends Biochem. Sci. 25, 381-388.
42. SOLIS, A.S., SHARIAT, N., PATTON, J.G. (2008) Splicing fidelity, enhancers, and disease. Front Biosci. 13, 1926-1942.
43. TARN, WY. Cellular signals modulate alternative splicing. J. Biomed. Sci. 14, 517-522.
44. TRAN, Q., COLEMAN, T.P., ROESSER, J.R. (2003) Human transformer 2beta and SRp55 interact with a calcitonin-specific splice enhancer. Biochim. Biophys. Acta. 1625, 141-152.
45. TUFFERY-GIRAUD, S., SAQUET, C., CHAMBERT, S., CLAUSTRES, M. (2003) Pseudoexon activation in the DMD gene as a novel mechanism for Becker muscular dystrophy. Hum Mutat, 21, 608-614.
46. VALCARCEL, J., GREEN, M.R. (1996) The SR protein family: pleiotropic functions in pre-mRNA splicing. Trends Biochem. Sci. 21, 296-301.
47. WILTON, S.D., FALL, A.M., HARDING, P.L., MCCLOREY, G., COLEMAN, C., FLETCHER, S. (2007) Antisense oligonucleotide-induced exon skipping across the human dystrophin gene transcript. Mol. Ther. 15, 1288-1296.
48. ZHENG, Z.M. (2004) Regulation of alternative RNA splicing by exon definition and exon sequences in viral and mammalian gene expression. J. Biomed. Sci. 11, 278-294.
49. ZHU, J., MAYEDA, A., KRAINER, A.R. (2001) Exon identity established through differential antagonism between exonic splicing silencer bound hnRNP A1 and enhancer bound SR proteins. Mol. Cell. 8, 1351-1361.

LEGENDS TO FIGURES

Figure 1

A) The genomic configuration of dystrophin intron 11 of the patient with XLDC. Nucleotides numbers refer to accession no. y13186. 5' ss and 3' ss indicate the canonical splice sites; 3' css and 5' css indicate the cryptic splice sites. The vertical arrow indicates the deletion breakpoint. The grey box represents the LINE1 element (L1M1_5) containing 136 bp of the *Alu*-exon and the ESE and SRB splicing motifs. The complete sequence of the *Alu*-exon is shown below the graph. The ESE motif is underlined and the Mse I restriction sites are boxed. The bigger bold letters indicate the cryptic splice sites recognized in the M3 splicing product (Fig. 2, A and B). The complete sequence of the SRB region is shown above the graph. **B)** MUA parental mini-gene graphic representation. Nucleotides numbers refer to accession no. y13186. 5' ss and 3' ss indicate the canonical splice sites; 3' css and 5' css indicate the cryptic splice sites; *Alu*-exon is boxed; dotted boxes and dotted lines represent β-globin exons (2 and 3) and intronic regions; ESE and SRB precise positions are also shown. **C)** MUA-ΔE mini-gene derives from MUA mini-gene by deleting the 15 nucleotides containing the ESE motif. D) MUA-ΔSRB mini-gene derives from MUA mini-gene by replacing the SRB sequence with a neutral lambda stuffer of the same size.

Figure 2

A) *In vitro* splicing assays of MUA and MUA-ΔE transcripts. *In vitro* splicing assays at incubation times of 0, 0.5, 1, 2, and 3 hrs. The schemes of lariat molecules and splicing products are shown on the sides. M0 indicates the two unspliced transcripts of 1372 bp and 1357 bp; M2: a 437 bp splicing product including the *Alu*-exon spliced between β-globin exon2 and exon3; M3: a 344 bp splicing product consisting of a 66 bp novel exon spliced between exon2 and exon3 of rabbit β-globin gene. The M3 splicing product is generated by the recognition of two different cryptic splice sites within the *Alu*-exon (see Fig.1, Panel A), the 3' splice site is located 4 nucleotides downstream the one used by the *Alu*-exon, and the 5' splice site 74 nucleotides upstream the 5' splice site of the *Alu*-exon; B1: the canonical splicing produtct joining rabbit β-globin exon 2 to exon 3; and B2: the β-globin exon 2.

B) *In vitro* splicing assays of MUA and MUA-ΔSRB transcripts. The autoradiography illustrates the in vitro splicing products of MUA and MUA-ΔSRB transcripts at incubation times of 0, 0.5, 1, 2, and 3 hrs. The schemes of lariat molecules and splicing products are shown on the left. M0 indicates the 1372 bp unspliced transcript; M2: a 437 bp splicing product including the *Alu*-exon spliced between exon2 and exon3 of rabbit β-globin gene; M4: a 330 bp aberrant splicing product

joining β-globin exon 2 to two copies of β-globin exon 3; B1: the canonical splicing produtct joining rabbit β-globin exon 2 to exon 3; B2: the β-globin exon 2.

Figure 3

Immunofluorescence characterization of MyoD-infected fibroblasts

In order to assess the myogenic differentiation induced by infection with recombinant adenoviral vector carrying the MyoD gene, samples were double-labeled with monoclonal antibodies against desmin (TRITC, A) or developmental myosin heavy chain (FITC, D, C, D). Polynucleated myotubes were obtained after 7-10 days of culture in differentiation medium (C,D).

Figure 4

Immunofluorescence analysis of dystrophin in patient myogenic cells

Double labeling for developmental myosin heavy chain (green, A, C) and dystrophin (red, B, D) of Myo-D transformed patient derived fibroblasts revealed the rescue of dystrophin expression either in untreated (B) and in AON-treated (D) cells.

High magnification (100X) demonstrated the correct protein localization at the sarcolemma.

Figure 5

Real Time RT-PCR quantification of *Alu*-exon skipping.

A) Percentage of AONs-induced *Alu*-exon skipping at 100 nM AON concentration. Transcriptional analysis was performed in AON-treated (100 nM) patient derived myogenic cells in comparison with untreated cells. Exon specific RealTime PCR assays were designed on dystrophin exon 10, 12 and *Alu*-exon. Histograms represent the relative quantification of the percentage of specific AON-induced *Alu*-exon skipping. ESEN1, ESEN2, SRBN3, SRBN4, SRBN5, SRBV1 and SRBV2, indicate the AON (see Table 2).

B) Percentage of AONs-induced *Alu*-exon skipping at concentrations ranging from 50 to 100 nM. Histograms represent the relative quantification of the percentage of specific *Alu*-exon skipping induced by the two more effective AONs, ESEN2 and SRBN3, tested at different concentrations.

Table 1

Oligo ID	Sequence (5'-3')	Orientation	Reference sequence	Position (nt)

			(accession no.)	
DysgenA*	ATTCATGTTATATGGTCGACCATGGTC ATGAGAATGGATTATCTC	forward	y13186	2184-2208
PlinC*	GTTAGCAGAGTCGACATTGAGGTACC GGTTTCGATTGGCATGGAATACTTG	reverse	y13186	3153-3129
MUAF*	ATTCATGTTATATGCATATGGTTTAAG TCCTTAACGTACC	forward	y13186	2971-2952
MUAR*	GTTAGCAGACATATGATTCTTATTAAT TTTTATGTACC	reverse	y13186	2817-2839
LambdaF2*	ATTCATGTTATATGCATATGAGCGTAT TAGCGACCCATCG	forward	NC_001416.1	23449-23468
LambdaR2*	GTTAGCAGACATATGTTGGGCTAAAA ATTCTCGC	reverse	NC_001416.1	23698-23680
T7Ex2	AAATTAATACGACTCACTATAGGGCT GCTGGTTGTCTACCCA	forward	J00659	701-720
Ex2F	GGCTGCTGGTTGTCTACCCA	forward	J00659	701-720
Ex3R	AACTTACCTGCCAAAATGATGAGACA	reverse	J00659	1544-1526

Footnotes: The asterisk indicates primers modified in their 5' end for cloning procedures.

Table 2

AON	Sequence	Mapping (Y13186)
ESEN1	uucuuuaagauugaagaacgcc	2430-2409
ESEN2	cauccuuuucuuuaagauug	2437-2418
SRBV1	cuuaaacacuucccauuuug	2958 -2939
SRBV2	ucauucucucuuuccuucgug	2904-2887
SRBN1	uuacuauuaaugaaaguaauuuu	2881-2859
SRBN2	uuuugcuauuuccuuucugguug	2943 - 2921
SRBN3	uuaucauugguacguuaaggacu	2979-2957
SRBN4	uuuuauguaccugaguacauu	2827-2807
SRBN5	ccuuucugguuguuuuguggcc	2932 - 2911

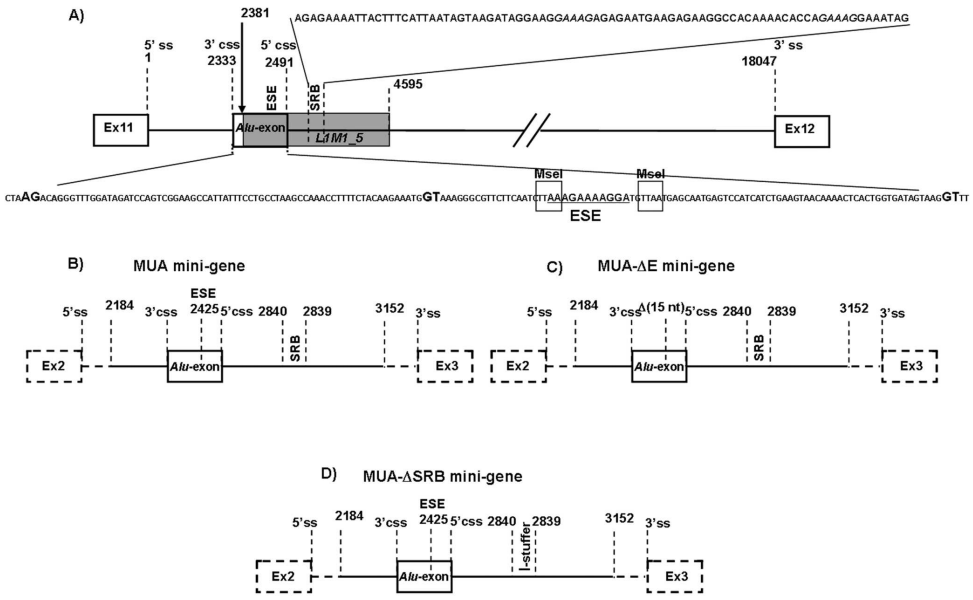

90x58mm (600 x 600 DPI)

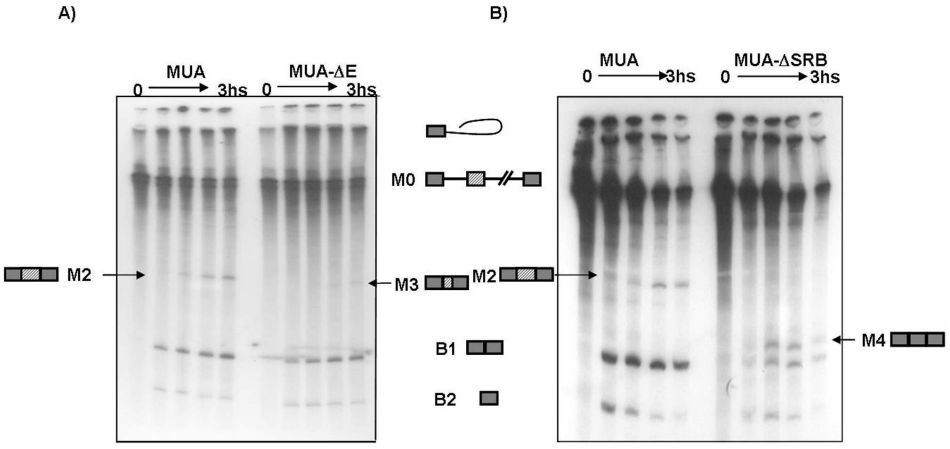

180x92mm (300 x 300 DPI)

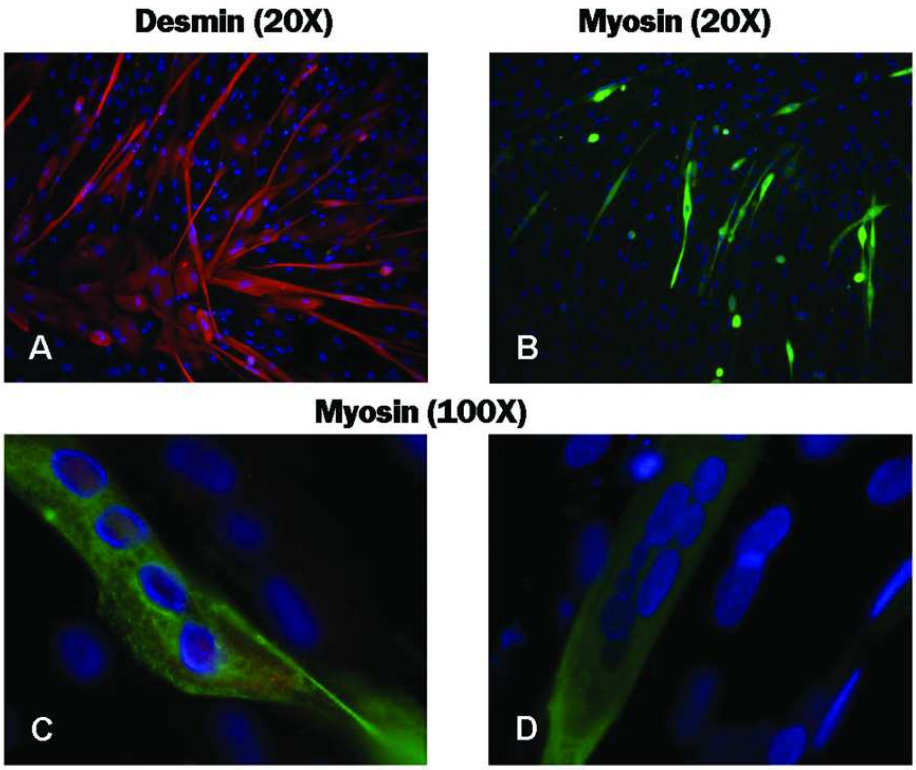

80x65mm (300 x 300 DPI)

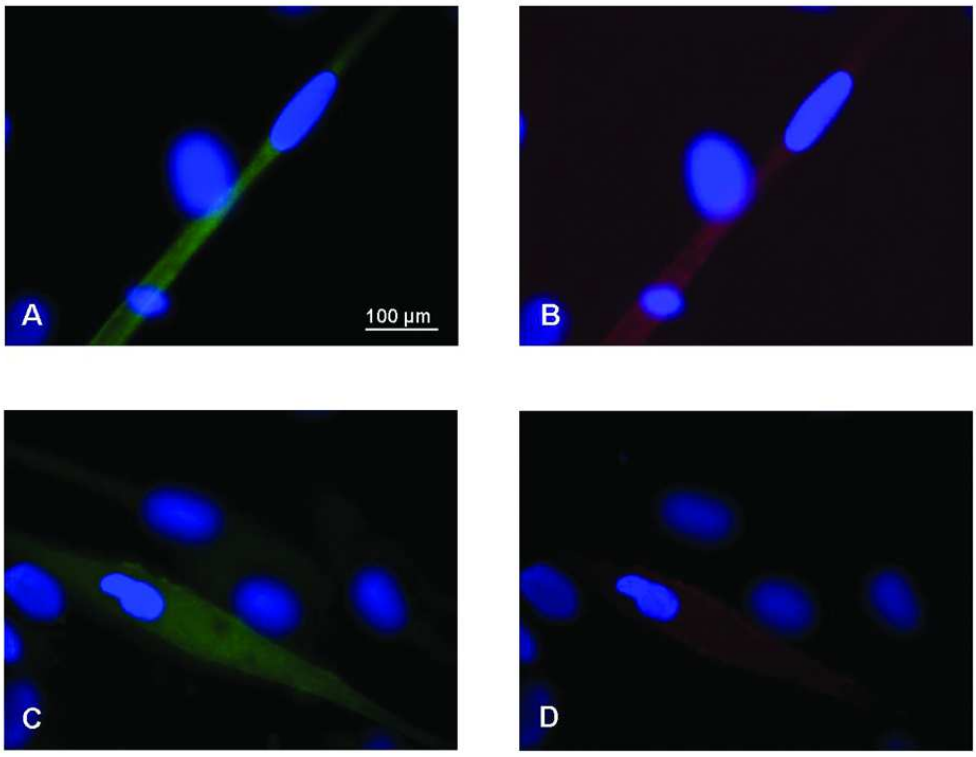

80x62mm (300 x 300 DPI)

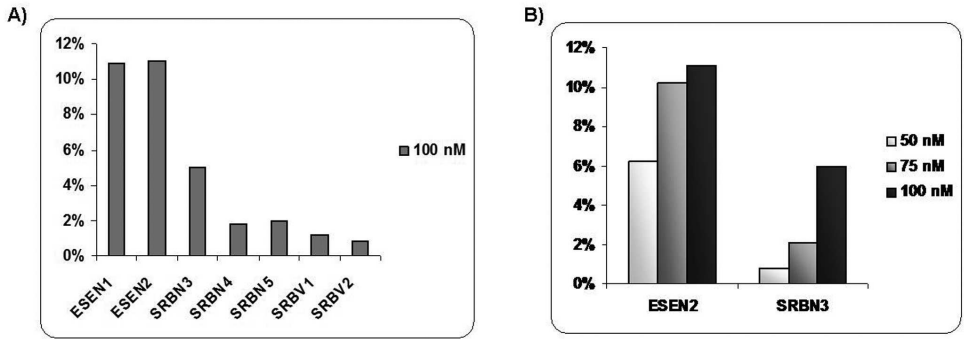

180x68mm (300 x 300 DPI)